Force-Mediated Adhesion Strengthening in Endothelial Cells at Adherens Junctions

by

Anita S. Kris

S.B. Materials Science and Engineering
S.B. Biology
Massachusetts Institute of Technology, 2006

SUBMITTED TO THE DEPARTMENT OF BIOLOGICAL ENGINEERING IN
PARTIAL FULFILLMENT OF THE REQUIREMENTS FOR THE DEGREE OF

MASTER OF ENGINEERING IN BIOMEDICAL ENGINEERING
AT THE
MASSACHUSETTS INSTITUTE OF TECHNOLOGY
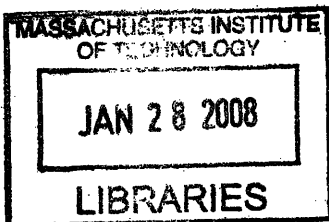
SEPTEMBER 2007

Signature of Author: _____

Anita S. Kris
Department of Biological Engineering
September 4, 2007

Certified by: _____

Roger D. Kamm
Professor of Mechanical Engineering and Biological Engineering, MIT
Associate Head, Department of Mechanical Engineering, MIT
Thesis Supervisor

Certified by: _____

Alisha L. Sieminski
Assistant Professor of Bioengineering
Franklin W. Olin College of Engineering
Thesis Supervisor

Accepted by: _____

Bevin P. Engelward
Associate Professor of Biological Engineering
Chair, Master of Engineering in Biomedical Engineering Program

Force-Mediated Adhesion Strengthening in Endothelial Cells at Adherens Junctions

by

Anita S. Kris

Submitted to the Department of Biological Engineering
On September 4, 2007 in Partial Fulfillment of the Requirements for the
Degree of Master of Engineering in Biomedical Engineering

Abstract

Cells respond to the application of force with a variety of biochemical responses modulating their shape, structure, function, and proliferation. Two force-responsive links between the inside and outside of a cell are integrin proteins, which link a cell to the extracellular matrix (ECM), and cadherin proteins, which link neighboring cells to each other. The strength of integrin-ECM bonds has been noted to increase in response to the application of force. However, the strengthening of cadherin-cadherin bonds in response to force has not been studied. Here, we use magnetic trapping to probe adhesion strengthening at cadherin adherens junctions, using cadherin-coated magnetic beads to simulate neighboring cells and apply force at adherens junctions. 43% of beads exposed to a high force (2.1 nN) detached, compared to 31% of those exposed to a low-to-high force ramp followed by high force. This indicates that adherens junctions are strengthened by force application. The actin cytoskeleton and vasodilator-stimulated phosphoprotein (VASP) both associate with adherens junctions, so their role in adhesion strengthening at adherens junctions was also studied. Cells treated with actin-inhibitor cytochalasin D showed no difference in bead detachment from constant high force and from ramped followed by high force, indicating that the actin cytoskeleton is crucial in the adhesion strengthening response. Beads attached to cells expressing GFP-VASP, which behave like VASP-overexpressing cells, detached in 24% of trials when exposed to constant high force, compared to 39% of trials in response to ramped force. Cells expressing GFP-MITO-FPPPP, which behave like VASP-downregulated cells, showed no difference in bead detachment between application of high force and ramped force followed by high force. These experiments indicate that VASP is necessary for the adhesion strengthening response, but high levels of VASP may slow actin restructuring and diminish the ability of the cytoskeletal linkages to respond to increasing force. The importance of VASP in cells' responses to forces from other cells suggest that modulation of VASP activity may play a role in tissue development, where cell-cell force responses are important, and the pathogenesis of certain diseases, where cell-cell adhesion is affected.

Thesis Supervisor: Roger D. Kamm, Ph.D.
Title: Professor of Mechanical and Biological Engineering
    Associate Head, Department of Mechanical Engineering

Thesis Supervisor: Alisha L. Sieminski, Ph.D.
Title: Assistant Professor of Bioengineering
    Franklin W. Olin College of Engineering

Table of Contents

1.0 Introduction

Within tissues, the shape, organization, and phenotype of cells are influenced by mechanical forces[1]. Forces can be applied to a cell by other cells, the extracellular matrix, or the environment. This thesis focuses on the response of endothelial cells to forces exerted by neighboring attached cells. Specifically, it investigates the possibility that the application of force at a cell-cell contact triggers active cell processes which increase the strength of cell-cell adhesion. This introduction reviews the structure of the endothelium is reviewed, followed by the ways endothelial cells form attachments to the extracellular matrix and to each other. The effect of forces on endothelial cells as they are presently understood are reviewed, focusing on mechanotransduction through cell-cell and cell-ECM contacts.

1.1 The Endothelium

Blood vessels are lined with a thin layer of specialized, closely apposed squamous epithelial cells, called endothelial cells, which together constitute the endothelium. The endothelium is a semi-permeable barrier for solutes in the bloodstream. Nutrients and white blood cells pass across the endothelium to enter tissues when needed, while large molecules like blood plasma proteins are blocked[2]. Endothelial cells respond to a variety of environmental stimuli, such as cytokines, hemodynamic forces, bacterial products, viruses, hypoxia, and increased concentrations of blood components with the induction of various genes, a process known as endothelial activation. Genes upregulated in endothelial activation include adhesion molecules, cytokines, growth factors, and relaxing and contracting factors that can affect the underlying smooth muscle cells[3]. Endothelial activation is the bridge between the state of the bloodstream and its effect on the body. For example, shear stress in the bloodstream and acetylcholine are two stimuli that lead

muscle cells to allow the vasodilation response, expanding the blood vessels and thus decreasing blood pressure[4]. Another response induced by shear stress on cells is cytoskeletal restructuring. Blood flow in the vessel induces the endothelial cell to change from polygonal to ellipsoidal and to elongate in the direction of flow[5]. The shape change is accompanied by the organization of F-actin in the cell from being diffusely distributed in the cell into dense fibers oriented perpendicular to the direction of flow, and upregulation of E-selectin, an intercellular adhesion molecule[6].

Proper endothelial activation is dependent on the structural integrity of the endothelium[7]. The integrity of the endothelium is maintained through the attachment of the cells to their underlying extracellular matrix (ECM) and to each other. Fundamentally, three types of proteins are involved in these attachments:

1) **Cell adhesion molecules (CAMs)** which span the cell membrane and mediate binding at the extracellular surface of the cell,

2) **ECM proteins**, large glycoproteins which can be bound tightly by specific cell adhesion molecules and adhesion receptors, and

3) **intracellular linker proteins**, which connect CAMs to the cytoskeleton, regulate the function of the CAMs, and transduce signals sensed by the CAMs at the cell surface into responses inside the cell.

Complexes of these proteins form the fundamental units of cell adhesion, linking the cytoskeleton to the outside of the cell[8]. For endothelial cells, the fundamental unit of adhesion between the cell and ECM is the focal adhesion, while the analogous unit of adhesion linking cells to each other is the adherens junction[9].

1.1.1 Focal adhesions

In focal adhesions, the binding of the surface of the cell to the ECM is mediated by

the integrin family of cell adhesion molecules. Integrins are transmembrane heterodimeric glycoproteins which bind to ECM proteins at their extracellular domain and to cytoplasmic linker proteins such as paxillin, talin, vinculin, zyxin, and α-actinin at their intracellular domain. Endothelial cells produce multiple integrins with differing sets of α /β subunits, allowing a variety of ECM proteins to be bound, such as collagen, laminin, fibronectin, and vitronectin[10]. So far, more than 60 cytoplasmic proteins have been identified as components of focal adhesions. Integrin does not bind actin directly; rather, a subset of these cytoplasmic proteins forms a structural link between integrin and actin. Other cytoplasmic proteins at focal adhesions are enzymes which are activated by binding to the structural proteins in focal adhesions[11].

1.1.2 Adherens junctions

In adherens junctions, the relevant cell adhesion molecule is cadherin. Different cell types express cadherins with different but homologous structures; the form expressed by vascular endothelial cells is known as VE-cadherin (for "vascular endothelial-cadherin"). Cadherins have an extracellular domain, a single-pass transmembrane region, and a cytoplasmic tail. The extracellular domains of cadherins consist of five identical repeating subdomains, labeled EC1 through EC5, linked and stabilized by calcium ions that bind the base of each subdomain to form a rigid, rodlike structure. Two adjacent cadherins on the surface of a cell dimerize laterally, and these homodimers bind to cadherin homodimers on other cells[5]. On the intracellular side, VE-cadherin associates with both the actin cytoskeleton and intermediate filaments through cytoplasmic linker proteins. The intracellular domain of cadherin binds to the cytoplasmic plaque proteins β-catenin, plakoglobin, p120, and p0071. β-catenin and plakoglobin bind to α-catenin, which in turn binds to actin, thus completing the link between the actin cytoskeleton and the adjacent cell.

Plakoglobin and p0071 bind to desmoplakin, which binds to vimentin intermediate filaments[12] (Figure 1.1). Additionally, many of the same intracellular proteins associated with focal adhesions have also been found in adherens junctions.[13]
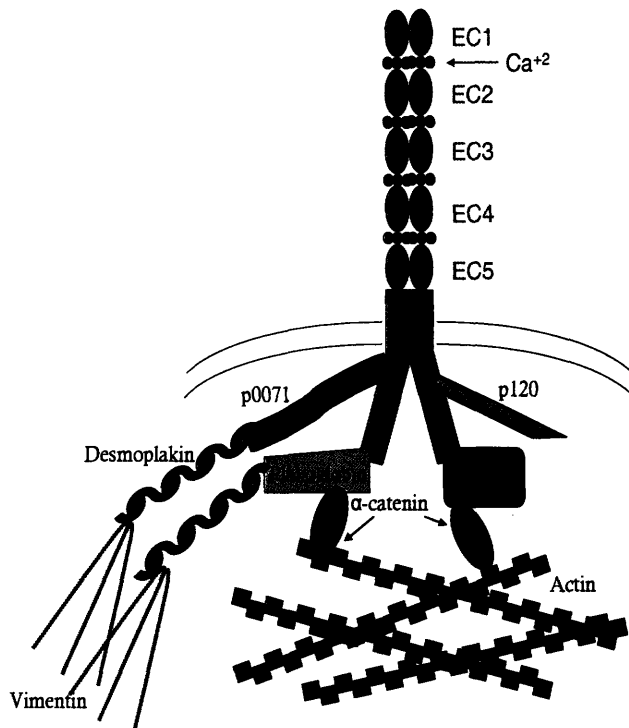
Fig. 1.1 .Schematic representation of intracellular linkage between VE-cadherin and the actin and intermediate filaments in the cytoskeleton [drawing based on Ref. 9].

1.2   Mechanosensing in the Endothelium

Mechanical forces play an important role in structuring the endothelium. As discussed in 1.1, shear stress influences the shape and orientation of cells. Mechanical forces can also cause dysfunction in blood vessels, as in atherosclerosis, characterized by the formation of protruding lesions on the vascular lumen that can lead to the occlusion of blood vessels or the weakening and rupture of the blood vessel wall. Atherosclerosis is induced in bifurcating and branching points in blood vessels, where blood flow is turbulent, as opposed to the laminar flow in straight sections of blood vessels. The cells in the laminar regions

produce molecules promoting a vasoactive, anticoagulant, anti-inflammatory, and growth-inhibitory surface, whereas in turbulent regions, a proliferative, prothrombotic, and adhesive phenotype is induced[14].

In both the cytoskeletal restructuring responses to forces from flow and the evolution of atherosclerosis, mechanical signals from outside the cell are transduced to biochemical signals inside the cell, promoting cytoskeletal restructuring, cell division, modulation of cell adhesivity, and release of cytokines and growth factors. Many of these responses are induced by the activation of shear responsive molecules on the cell membrane. These include members of the receptor tyrosine kinase family, calveolae (small invaginations of the membrane), stretch-activated calcium ion and potassium ion channels, G proteins, and G protein-coupled receptors[15]. Also involved in the transduction of external mechanical signals are integrins and cadherins, which, through their bridging to the cytoskeleton and their association with signaling pathways, can effect biochemical and mechanical change in the cell[16].

1.2.1 Mechanotransduction at focal adhesions

Focal adhesions transmit mechanical forces from the matrix to the cell, inducing biochemical activity. The application of mechanical stretching at focal adhesions causes the binding of several proteins to the focal adhesion, such as paxillin and focal adhesion kinase (FAK)[17]. Many proteins that localize to focal adhesions, including FAK, are activated through autophosphorylation upon stretching, and then act on downstream targets which can influence cell processes.[18] For instance, activation of FAK leads to degradation of proteins p21/Cip and p27/Kip, leading to the promotion of cell proliferation and the inhibition of apoptosis[19],[20].

Each adherent cell forms numerous adhesions to the ECM, and information about the mechanical properties of the ECM are transmitted through the focal adhesions and

transduced into signals to determine cell shape and spreading. For instance, in vitro experiments showed that the area of cell spreading depends on the density of ECM proteins.[21]. The area over which a cell spreads, in turn, affects cell proliferation, as increased cell spreading increases tensile forces in the actin cytoskeleton[22], which in turn act on proteins needed for cell cycle progression[23]. The maintenance of tensile forces through focal adhesions is also important for migration. Cells sample the stiffness of the ECM at focal adhesions and through a FAK-mediated process migrate toward the region of greatest stiffness[24],[25].

1.2.2 Mechanotransduction at adherens junctions

The transduction of force through cell-cell contacts is essential for tissue development and affects the biochemical and mechanical properties of cells. Load bearing tissues in cadherin knockout animals exhibit malformation during development[26], because physiological force application is crucial in tissue structuring, and cell-cell mechanotransduction is also essential to the formation of specialized layers of cells within tissues[27]. Recent experiments seeding fibroblasts on flexible N(neural)-cadherin-coated elastomer pillars show that the traction forces exerted through cadherin contacts reaches 50 nN, comparable to the force levels exerted by focal adhesions[28]. Use of fluorescent microbead rheometry showed that forces exerted by one fibroblast through an adherens junction can cause viscoelastic deformation and elongation of actin bundles in the neighboring cell[29], showing that cells change respond with active biological restructuring to mechanical force at cell-cell contacts.

One mechanism by which mechanotransduction may occur at cell-cell contacts is through the activation of stretch-sensitive calcium ion channels by forces at cadherins. Magnetic beads coated in anti-N(neural)-cadherin-antibody were attached to fibroblasts to bind N-cadherin at the cell surface. Application of magnetic forces to the beads induced

robust transient currents of Ca+2, a 2nd messenger involved in actin filament assembly and turnover, and ultimately increased the amount of polymerized actin in the cell, potentially explaining force-mediated viscoelastic response[30].

Another important role of tension at adherens junctions may be cell cycle and protein production control. β-catenin binds to cadherin in the adherens junction, but when it is dissociated it can translocate to the nucleus and upregulate genes involved in the cell cycle[31]. One example is the upregulation of survivin, an apoptosis-inhibiting protein that promotes cell division. In confluent endothelial cells where VE-cadherin adherens junctions are intact, levels of survivin are low. Cells with null or dismantled VE-cadherin have high levels of survivin, as presumably β-catenin is upregulating survivin[32]. Tension at adherens junctions may control the fractions of bound versus dissociated β-catenin, though a direct correlation of force application and β-catenin recruitment has not been demonstrated.

1.3   Adhesion Strengthening

Adhesion strengthening is the process by which an adhesion, initially formed by the attachment of an integrin to an ECM protein or a cadherin to another cadherin, becomes more difficult to break. One observed behavior in focal adhesions, described more fully in the following section, is adhesion strengthening in response to applied force. Force-mediated adhesion strengthening has not yet been described in adherens junctions. However, the similarities of adherens junctions to focal adhesions indicates that force-mediated adhesion strengthening may occur at adherens junctions, and this possibility is supported by some preliminary evidence.

1.3.1 Force-mediated adhesion strengthening at focal adhesions

Adhesion strengthening was initially noted in experiments by Lotz et al. observing

the increase in adhesion force of fibroblasts and glioma cells to a fibronectin surface proportional to the time the initial contact was formed. The adhesion strength was further found to be proportional to the area of cell-substrate contact, and cells treated with cytochalasin B to disable actin polymerization and microfilament formation did not show a strengthening response, although they were able to form the initial adhesion. The authors proposed a three-component model of adhesion strengthening that is still accepted. Following the initial attachment of cell-surface integrins to ECM proteins, an adhesion is strengthened by (i) increased clustering of integrins, (ii) formation of protein interactions linking integrins to the cytoskeleton, and (iii) cell spreading to increase the area of contact[33],[34].

Force-responsive adhesion strengthening was noted in an experiment by Sheetz and colleagues involving optical trapping of fibronectin-coated beads attached to fibroblasts. The beads crawled freely across the surface of the cell, until a controlled amount force was applied for 1.5 seconds via laser to stop the crawling of the bead, mimicking force applied through an ECM attachment. The force was then turned off and the bead allowed to resume crawling across the surface. When the same force was again applied to the bead at a later time, the crawling of the bead was not stopped, indicating strengthening of the cytoskeletal linkages. For beads subjected to a longer initial force application period of more than 10 seconds, the cytoskeletal linkages became strong enough to free the trapped bead from the laser[35]. Further experiments showed that the application of force is required for the initial integrin-ECM bond to mature into a focal adhesion. Vinculin is recruited to integrin in response to force, and vinculin is needed for the cell to be able to exert forces to the ECM through the focal adhesion[36].

Signaling proteins have been found to be crucial to the maturation of focal adhesions. Among them is Rho, a G protein that localizes to focal adhesions and is involved in actin dynamics. Rho activates downstream targets like Rho-associated kinase (ROCK)

and mDia1 that are needed for force-responsive maturation of focal adhesions from dot-like membrane-matrix attachments into elongated structures that link to the cytoskeleton[37].

1.3.2 Preliminary evidence of force-mediated adhesion strengthening at adherens junctions

Though force-mediated adhesion strengthening has not been described at adherens junctions, there is some indication that adherens junctions may mature the way focal adhesions do in response to force. The formation of adherens junctions is similar to that of focal adhesions; there is an initial binding of the extracellular domain of the membrane protein, triggering the binding of the intracellular domain to cytosolic proteins, the recruitment of linker proteins, the enzymatic activation of some proteins, and ultimately the formation of a bridge of protein associations to the actin cytoskeleton. Many of the same cytosolic proteins are found at the two types of adhesions, including the actin-binding proteins zyxin, moesin, Arp2/3, and vinculin. Also, the same force responsive G proteins, such as Rho, Rac, and Cdc42, that are found at focal adhesions are found at adherens junctions[38].

Experiments assessing the time-dependence of cell-cell force support the idea that adherens junctions may mature similarly to focal adhesions. An assay using pipettes to separate cell doublets with a measured force found that the force needed to separate the cells increased with the amount of time they were in contact. As with focal adhesions, inhibiting the actin cytoskeleton pharmacologically blocked this strengthening response, though it did not affect the initial cadherin-cadherin binding[39]. The similar behavior of cell-cell behavior here to the cell-matrix adhesion observed by Lotz et al. implies that perhaps force would have a maturing effect on adherens junctions as it does on focal adhesions.

1.3.3 The role of VASP

The Ena/VASP proteins are a homologous family regulating cell migration and actin assembly[40]. The founding member of the family, *Ena*, was found in *Drosophila*; its knockout leads to defects in axonal architecture in the central and peripheral nervous systems[41]. In vertebrate endothelial cells, the relevant family members are vasodilator-stimulated phosphoprotein (VASP), Mena (Mammalian enabled), and EVL (Ena-VASP like). Ena/VASP proteins all have an N-terminal Ena/VASP homology 1 (EVH1) region, a proline-rich central region and a C-terminal Ena/VASP homology 2 (EVH2) region. The EVH1 region has binding sites for several of the proteins found in focal adhesions and adherens junctions, including zyxin and vinculin, and these proteins are thought to recruit Ena/VASP proteins to those locations. The central proline-rich domain binds to profilin, a G-actin-binding protein, and the EVH2 domain contains G-actin and F-actin binding sites as well as a site for Ena/VASP tetramerization[42].

Ena/VASP proteins may have multiple mechanisms of regulating actin dynamics. Ena/VASP proteins localize to the barbed ends of actin filaments, and appear to encourage the polymerization of actin by preventing capping proteins that inhibit polymerization from binding to actin[43]. VASP modulates the attachment of the cytoskeleton to the cell membrane, which is necessary for movement and force generation[44]. The distribution of VASP in the cell is force-respondent; VASP relocalizes from focal adhesions to actin filaments in the presence of mechanical stress[45]. Phosphorylation by protein kinase A (PKA) is one way the activity of Ena/VASP is modulated, as phosphorylation increases the activity of Ena/VASP proteins[46].

Experiments with mutant cell types devoid of Ena/VASP indicate that the family is vital for many actin-dependent processes, like cell migration and attachment, indicating that it may also be important in adhesion strengthening. In the bacterium *Listeria monocytogenes*,

knockout of Ena/VASP proteins disables interactions between cytoskeleton and the surface protein ActA, leading to an order of magnitude reduction in its speed within living cells. Knockout of simply the F-actin binding sites, G-actin binding sites, and profilin-binding sites leads to an increase in speed compared to wild-type Listeria, suggesting a complex role of Ena/VASP proteins beyond simply upregulating actin polymerization[47]. In fibroblasts, where Ena/VASP proteins are localized to the leading edge of the cell as well as to cell-cell and cell-matrix adhesions, knockout of Ena/VASP speeds cell migration, while upregulation of Ena/VASP slows it. This seemingly paradoxical observation is due to the regulation of actin geometry by Ena/VASP; actin filaments in the absence of Ena/VASP are shorter, more branched, and stiffer, and are subjected to less thermal fluctuation and Brownian motion than the longer, less branched actin filaments that form when Ena/VASP is present and capping proteins are inhibited. Thus, although actin filaments extend more quickly in Ena/VASP knockout fibroblasts, they are less persistent, causing an overall decrease in cell velocity[48]. In neurons, Ena/VASP proteins are necessary for proper axonal extension, and in the immune system they are important for phagocytosis by macrophages, chemotaxis of neutrophils toward bacteria, and the interaction of T cells with antigen-presenting cells[49].

Some experimental data support the importance of Ena/VASP proteins at cell-cell junctions in actin organization. VASP is recruited to adherens junctions at an intermediate point in the formation of adherens junctions[50]. In cells transfected with Mena, a member of the Ena/VASP family, two distinct pools of Mena were found inside adherens junctions: one associated with direct cadherin-actin connections, and another with actin bound to Arp2/3, an actin nucleator. Dislocation of Mena from either location disrupted the actin bundles bound there[51]. Given the importance of an intact actin cytoskeleton in force-mediated adhesion strengthening in focal adhesions, it is possible that one or both of the pools of Ena/VASP proteins would be important in adhesion strengthening in adherens junctions. Another piece of evidence comes from *in vivo* observations of mice lacking VASP, Mena,

and EVL. The mice showed vascular leakage and hemorrhaging during fetal development[52].
Further, endothelial cells lacking Ena/VASP function show increased permeability in an *in
vitro* assay while those over-expressing VASP show decreased permeability[527]. These
observations, taken in combination with the importance of cell-cell mechanotransduction in
developing load-bearing tissues normally[27], indicate that Ena/VASP proteins may be
important in properly forming and maintaining the strength of cell-cell junctions.

1.4   Magnetic trapping for biomechanical studies

Magnetic traps have been used previously to apply precise forces to cells to probe
mechanical properties and mechanotransduction.   Bausch et al. were the first to apply
magnetic trapping to the study of biomechanics, applying force to integrin-bound magnetic
beads and studying the local viscoelastic response[53].   Later experiments by Mack et al.
applied magnetic trapping to vascular endothelial cells, studying the translocation of focal
adhesions in response to shear force applied by the trap to ECM-linked magnetic beads[54].
Though magnetic trapping has not yet been used to probe cadherin function, Baumgartner et
al. used laser trapping of cadherin-coated beads to investigate the dependence of N-cadherin
function on calcium ion concentration in neurons[55].

1.5   Objective and motivation of study

These experiments attempt to verify the occurrence of force-responsive adhesion
strengthening at cadherin-cadherin contacts, and to examine the role of VASP and actin on
the ability of cells to strengthen adhesion.   We incubate cadherin-coated paramagnetic beads
with wildtype human endothelial cells *in vitro* to simulate cell-cell contacts *in vivo*. We then
use the magnetic trap to apply forces to the magnetic beads, thus imitating force application
from a neighboring cell.   To each bead, we apply either a low constant force, a high constant

force, or a low-to-high ramped force followed by constant high force, and we monitor the state of bead attachment. Our hypothesis is that, because of the similar proteins involved in focal adhesions and adherens junctions, their parallel functions as links between the extracellular environment and the cytoskeleton, and the influence of force application through both types of adhesions on cell processes, adhesion strengthening in adherens junctions is force-dependent; thus, a smaller fraction of the beads subjected to a ramping force and then constant high force will detach, compared to the beads subjected to constant high force alone.

As described in 1.3.3, the roles of VASP in actin dynamics have yet to be fully elucidated. We conduct our magnetic trapping experiments on human vascular endothelial cells stably transfected to express VASP linked to green fluorescent protein (GFP) in addition to the endogenously expressed VASP, functionally upregulating VASP. We expect the increased pool of VASP to increase adhesion strengthening as compared to wild type cells, reducing the proportion of cells detaching from ramped followed by constant high force. We also study adhesion strengthening in cells lacking Ena/VASP activity (caused by expression of an Ena/VASP binding motif localized to the mitochondria). We expect these cells to have a reduced strengthening response to the force ramp, and to see little difference between the cells exposed to a force ramp followed by high force and just high force.

Unlike VASP, the importance of actin in maturing adherens junctions has been demonstrated (as discussed in 1.3.2 and also demonstrated by El Sayegh et al.[56]) Whether actin's role in adhesion strengthening is force-respondent, however, has not been determined. We study the force-dependence of actin-based adhesion strenghthening by performing our magnetic trapping experiment on wildtype cells that are treated with cytochalasin D, a fungal protein which inhibits actin polymerization. Our hypothesis is that the overall strength of cadherin-cadherin adhesions will be lowered, and that the adhesion strengthening effect will also be lowered by reducing the ability of the adherens junction to

form linkages with the cytoskeleton, as was observed in integrin adhesion strengthening.

Our investigation is motivated by the hope of achieving a greater understanding of the physiological process of cell-cell adhesion. The loss of cell-cell adhesion, in addition to causing lethal deformities in the development of load-bearing tissues, has pathological consequences in fully formed tissues. Downregulation of E-cadherin has been observed in cancerous cells, potentially explaining the loss of contact inhibition of cell division and increased migration of tumors[57]. If loss of cell-cell adhesion is an important factor in the progression of cancer, reversal of that loss by upregulation of adhesion-promoting proteins could be a potential solution. Lowered cell-cell adhesion leads to tissue hyperpermeability, implicated in diverse conditions including ischemic retinopathies, pulmonary edema, inflammatory bowel disease, nephropathies, delayed hypersensitivity reactions, rheumatoid arthritis, and psoriasis[58]. Specifically in the vascular endothelium, septic and anaphylactic shock responses cause a rapid decrease in endothelial barrier function, causing systemic vasodilation, vascular leakage, and ultimately multiple organ failure due to hypoperfusion. Studying force-responsive adhesion strengthening could inform new ways to reverse the shock-induced loss of cell-cell adhesion.

2.0   Materials and Methods

2.1   Magnetic trap

2.1.1 Magnetic trap design

The magnetic trap was built after the design of Hayden Huang and Jan Lammerding

(described more fully in (59)). Briefly, the trap was a cylinder, 161 mm-long and 20 mm in

diameter, machined from CMI-C steel. The front 44 mm tapered to a 200 µm wide, 25°

chiseled rectangular tip. After mechanical damage to the trap, the tip became bent and was

filed down to a chiseled rectangular tip again, now approximately 250 µm wide. (The

damage and repair occurred before the experiments described in 2.4 were performed.) The 72

mm-long core was wrapped in eight layers of 18-gauge enamel-coated copper wire to create a

magnetic coil with approximately 400 turns total. The trap was mounted on a

micromanipulator to control its position. Current was provided to the copper coil by a

power supply (PSP-603, Instek, Taiwan) which resulted in a magnetic force at the tip of the

magnetic trap. The micromanipulator and microscope were mounted on a pneumatic

vibration isolation table to minimize forces from other sources. Figure 2.1 shows the setup

of the magnetic trap.

2.1.2 Magnetic trap calibration

Paramagnetic beads coated in protein A (100-01D, Dynal/Invitrogen), 2.8 µm in

diameter, were suspended in 70% ethanol and placed in a 60-mm polystyrene dish. After

evaporation of the ethanol in a laminar flow hood, the beads were resuspended in

dimethylpolysiloxane with a kinematic viscosity of 12,500 centistokes (DMPS-12M, Sigma).

The dish was placed on the microscope stage (Axiovert 200, Zeiss), the tip of the magnetic

trap was lowered into the dish, and the system was allowed to equilibrate for several minutes to stop residual motions. The tip was then brought into parfocal position with beads in the dish. The magnetic trap was operated at constant current in 0.5 amp steps from 1.0 to 3.5 amps, and videos were recorded of the motion over 150 to 200 µm by a high-speed camera (PCO.1200, PCO, Germany) at 25 frames per second and 50x magnification. These videos were then analyzed with particle-tracking MATLAB (Mathworks, Natick, MA) software developed by Jan Lammerding (1), yielding the position vs. time coordinates of the beads. The data were fit to a 9th degree polynomial using the Curve Fitting Toolbox in MATLAB and the derivative of this curve gave the velocity at each position. The force at each position was calculated from the velocity using Stokes' equation,

$$F = 3\pi\mu Du \qquad\qquad\qquad (Eq. 1),$$

where μ is the force, D the diameter of the bead, and u the velocity of the bead. To predict forces at distances greater than those measured directly by video, the force versus position data for each current level was fit to the phenomenological power law form $F = ax^{b} + c$, again using the Curve Fitting Toolbox.

The calibrations were corrected for the damage and repair noted in 2.1.1. After the tip was repaired, three bead-tracking experiments were performed at 1.0 A and another three at 3.5 A. Each experiment was fit as mentioned above to the power law form and the coefficients averaged to give the most accurate coefficients for bead tracking at these two currents. These power law coefficients were compared to those for bead-tracking experiments at the same current setting prior to the damage and repair of the magnetic trap. The amount of change in each coefficient was noted, and a linear equation for degree of correction versus current calculated for each coefficient a, b, and c, based on the degree of correction at 1.0 A and 3.5 A. Degrees of correction were extrapolated from these equations for the degree of correction of the coefficients in the 1.5 A, 2.0 A, 2.5 A, and 3.0 A bead

tracking experiments. The old power law data was modified with the degree of correction to give the force-distance correlation used in the magnetic trapping experiments below.

2.2   Bead coating and selection of appropriate coating density

The procedure for VE-cadherin coating of the 2.8 μm protein A-coated paramagnetic beads (the same beads used in force calibration in 2.1.2) was slightly modified from the manufacturer's instructions for the use of beads in immunoglobulin capture, and is similar to the process used by Baumgartner et al. for coating of beads with N-cadherin[37]. Protein A is native to bacterial cell walls and has a high specificity for binding immunoglobulins. A chimeric protein consisting of the extracellular domain of human VE-cadherin fused to the Fc region of human immunoglobulin G was used (938-VC, R&D Systems, Minneapolis, MN). The binding of the protein A on the beads to the Fc domain of the chimeric protein ensured that the extracellular domain of VE-cadherin was oriented radially outward and unhindered from interacting with VE-cadherin on cells. An imidoester cross-linker specific for primary amines, dimethyl pimelimidate (DMP·2HCl, Pierce Biotechnology, Rockford, IL), was used to secure the attachment of Protein A to the Fc domain while minimally impairing the activity of VE-cadherin.

The step-by-step procedure of coating is given in Appendix A. The beads were rinsed in a 100 mM sodium phosphate buffer before being incubated with a solution of the Fc/VE-cadherin chimeric protein for a controlled time period. Following the incubation, the beads were washed in 200 mM triethanolamine to remove unbound protein, and crosslinking with DMP followed. The crosslinking was quenched by washing the beads in 100 mM Tris. Finally, the beads were washed in Dulbecco's phosphate buffer solution (D-PBS) containing calcium and magnesium salts. As a minimum concentration of 2 mM Ca^{+2} is needed to maintain cadherin structure, all solutions used in the cell coating procedure

were prepared in D-PBS with Ca^{+2} and Mg^{+2}. After coating, the beads were stored in D-PBS at 4°C for up to 3 months before use.

The binding curve of the Fc domain to Protein A was calculated based on published kinetic data, and used to create beads with different coating densities by varying the time of incubation with Fc/VE-cadherin. These calculations are shown in Appendix B. Beads with 25%, 50%, 75%, and 100% of their available binding sites bound by the Fc/VE-cadherin protein were made. As a control, unreacted protein A coated beads were also used in experiments. These beads were tested for their potential use in bead pulling experiments in preliminary experiments. Cadherin-coated beads were incubated with HUVECs for different lengths of time, and the ability of the beads to detach from the cells in response to low and high force levels was examined. Incubation periods of 15 minutes, 30 minutes, 2 hours, and 24 hours were examined.

2.3   Cell Culture

Experiments investigating force-mediated adhesion strengthening on wild-type endothelial cells were performed with Human Umbilical Vein Endothelial Cells (HUVECs) (Cascade Biologics, Portland, OR). The cells were stored frozen in fetal bovine serum (FBS) with 10% dimethyl sulfoxide (DMSO) in liquid nitrogen. After thawing, cells were plated in collagen-coated 25 cm^2 tissue culture flasks, covered in media (EBM-2, Lonza, Basel, Switzerland) and cultured at 37°C with 5% CO_2.

For experiments assessing the effect of upregulation and downregulation of Ena/VASP family members on force-mediated adhesion strengthening, HUVEC cell lines that had been stably transfected with retroviral vectors coding for GFP-VASP or GFP-MITO-FPPPP were used (generous gift of Dr. Craig Furman, MIT). HUVECs transfected with GFP-VASP express a chimeric VASP protein attached to green fluorescent protein (GFP), in addition to expressing the endogenous VASP gene. The GFP-VASP protein acts

like normal VASP in terms of localization to focal adhesions and adherens junctions, leading to the overall effect of VASP upregulation in the cell[60],[61]. GFP-MITO-FPPPP cells express a mitochondrial protein with an FPPPP motif that is tightly bound by the proline-rich central region of Ena/VASP family members. The result is recruitment of Ena/VASP proteins to the mitochondria and away from the plasma membrane, resulting in functional disabling of the role of Ena/VASP in organizing actin[62].

For all experiments, cells at passage 5, 6, or 7 were trypsinized and plated in 35-mm diameter polystyrene tissue culture dishes coated in collagen. 10,000 to 20,000 cells were transferred to each dish. The dishes were covered in 2 mL fresh media and returned to the incubator. Experiments were performed 12 to 24 hours after plating.

2.4   Force-mediated adhesion strengthening experiments

2.4.1 Magnetic trap force application to VE-cadherin-coated beads attached to wild-type HUVECs

Prior to each experiment, a single HUVEC-plated tissue culture dish would be removed from the incubator. 0.5 mL media were withdrawn from the dish and placed in an Eppendorf tube. The cadherin-coated beads in D-PBS were removed from 4°C storage and Vortexed vigorously to suspend them and break up bead-bead adhesions. A small volume of the suspension containing approximately 10,000 magnetic beads were added to the media in the Eppendorf tube. The beads were mixed with the media by pipetting in the Eppendorf tube and then gently added back to the dish to distribute the beads well while minimizing force application to the cells. The dish was returned to the incubator for 40 to 50 minutes until the start of the experiment.

An aluminum plate connected to resistive heaters was placed on the microscope stage and preheated to maintain the media at 37°C. A hole was placed in the plate to allow

observation via the microscope objectives of the cells located in the inner 25 cm of the dish's diameter, while the 5 cm periphery of the dish was in direct contact with the heating plate. The dish was removed from the incubator and placed on the aluminum plate.

Cells which were not in contact with other cells and had only one magnetic bead attached to them were identified under the microscope. At a distance of approximately 250 μm from the bead, a current of 1.0 A was applied for five seconds to the copper coil wrapped around the magnetic trap, and the resulting movement of the bead observed. Beads that did not appear to move in response to this force were considered sufficiently adhered for the experiment. The tip of the magnetic trap was next brought into parfocal position by eye with a suitable adherent bead and positioned approximately 30 μm away from the bead by eye. Due to camera malfunction, this distance could not be precisely placed using live video imaging, so the use of slide rulings and the diameter of beads in the solution were used to help estimate a distance of 30 μm from the bead to the tip.

A magnetic force was applied to the adherent bead via the activation of current. The beads were subjected to one of three force conditions: either 1) the application of 1.0 A for 110 seconds, 2) the application of 3.5 A of current for 110 seconds, or 3) the application of current ramped from 1.0 A to 3.5A in 0.5 A steps changing every 10 seconds for 50 seconds, followed by a constant force of 3.5 A. The application of currents for the specified periods of time was controlled via the RS-232 serial communication standard by a a laptop running custom-written Matlab codes, presented in Appendix C. The state of attachment of each bead was noted througout the course of the experiment, with the time of detachment recorded in cases where detachment occurred. Subsequent tests were conducted on cells that were at least 500 μm away from previously tested cells to avoid confounding prestressing forces from previous tests. Dishes were searched left to right in rows starting from the upper left corner to further avoid confounding prestressing forces (as force was applied from right

to left). Individual dishes were used for a maximum of 30 minutes to minimize the effects of

lowered CO_2 and less stable temperature control in the ambient air as compared to the

incubator.

2.4.2 Force-mediated adherens junction strengthening in Ena/VASP variant HUVECs

Magnetic trapping experiments identical to those on wild-type HUVECs were

performed on the GFP-VASP and GFP-MITO-FPPPP transfected cell lines.

2.4.3 Actin inhibition and force-responsive strengthening of adherens junctions

Cytochalasin D from Zygosporium masonii (C8273, Sigma) was used to investigate

the role of actin in strengthening of adherens junctions. The lyophilized cytochalasin D was

dissolved in dimethylsulfoxide (DMSO) (D8418, $\geq 99.9\%$, Sigma) to yield a 10 mM stock

solution. The stock solution was stored at -20°C, and diluted to 10 µM in D-PBS without

Ca^{+2} and Mg^{+2}. Immediately after addition of VE-cadherin-coated beads to a dish as

described in 2.4.1, 38 µL of the 10 µM solution were added to the media (on average, 1.9 mL

due to some evaporation in the incubator) to bring the concentration of cytochalasin D in the

dish to 200 nM.

The dishes were returned to the incubator for 40-50 minutes as in the wild-type and

Ena/VASP variant experiments, and bead trapping experiments identical to those in 2.4.1
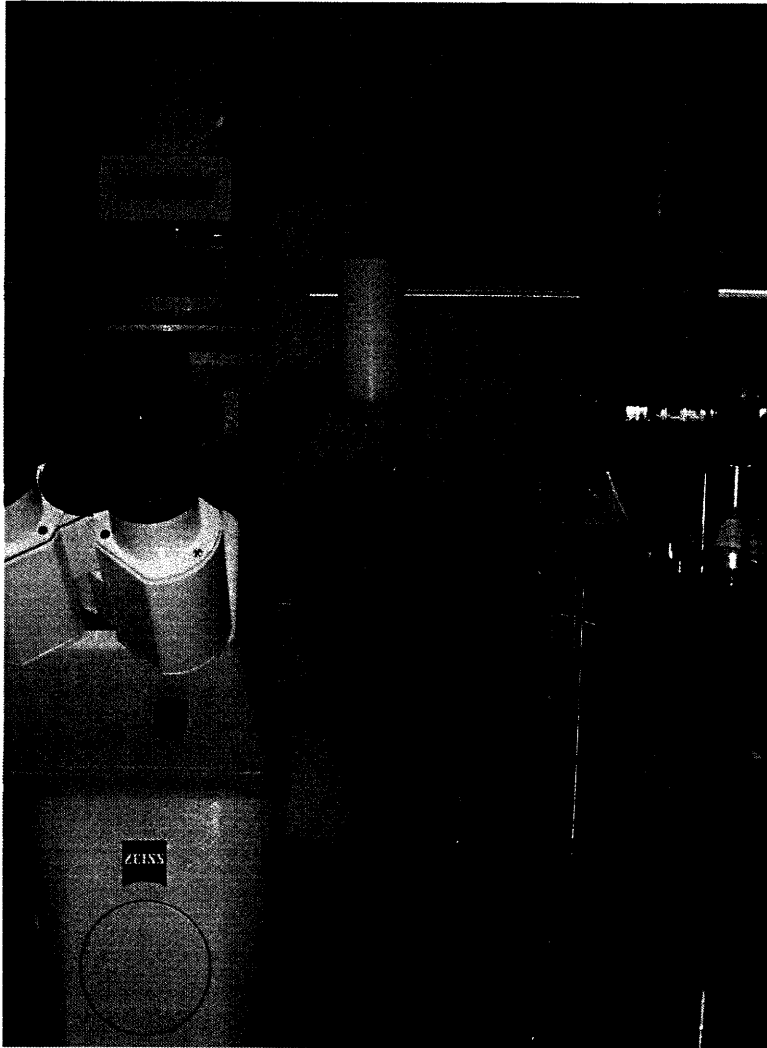
and 2.4.2 were performed on the cells.

Fig. 2.1. The setup of the magnetic trap, micromanipulator, and microscope on a vibration-controlled table.

3.0   Results

3.1   Force calibration and applied force profiles

Fitting the data from the measurements of magnetic bead tracking in DMPS to

power law form, corrected for the effects of damage and subsequent repair, yielded

reasonable relationships between current, distance from the tip of the magnetic trap, and

force. At a fixed distance of 30 μm, the force-current relationship is nearly linear. (Figure

3.1). The power law fits can be extrapolated to find the forces applied in the bead pulling

experiments described in 2.4.1 - 2.4.3. Because the 30 μm distance was placed by eye, an

error of up to 10 μm in tip placement is considered (Figure 3.2). However, 5 μm is a more

likely error in tip placement. At either error level, the difference at the extreme ends of the

error bars between the low force profile (1) and the high force profile (2) are still very large.

For instance, for force profile 3 the power law fit predicts that the force applied is 2.1 nN. A

10 μm error in tip placement could lead to a difference of about 700 pN from this force,

while a 5 μm error in tip placement could lead to an difference of about 300 pN.

3.2   Bead density selection and non-cadherin coated bead control experiment

The different beads prepared according to 2.3 were tested for their potential use in

bead pulling experiments in preliminary experiments by incubating the beads with HUVECs

for different lengths of time and assessing their response to low (690 pN) and high (2.1 nN)

force applied by the magnetic trap (Table 3.1).   Beads coated at 75% or 100% density

formed very strong attachment to the cells in just 15 minutes that could not be broken with

high force, while the 25% coated beads did not form attachments in a 15 minute incubation

resistant to low or high forces. 25% and 50% coated beads incubated with cells for either 30

minutes or 2 hours displayed more detachment in response to higher force and less detachment in response to lower force.

The binding of cadherin-coated beads appears to trigger endocytosis in the cells. At later timepoints, beads could be seen inside the cell. For any given timepoint, the fraction of cells with endocytosed beads was higher for beads more densely coated with cadherin. Thus, endocytosis of the beads appears to occur at rates proportional to the density of cadherin coating. Partially endocytosed beads (having a non-spherical appearance due to partial engulfment by the cell membrane) were also visible. To minimize the fraction of endocytosed beads during experiments, 25% cadherin-coated beads were chosen for the adhesion strengthening experiments.

Interestingly, VE-cadherin-coated beads adhered as strongly to the bottom of dishes as they did to the cells, with most beads coated at greater than 25% cadherin density totally immobile in response to forces over 2 nN. The extracellular domain of cadherin is considered to only participate in homophilic binding with other extracellular cadherin domains; direct adhesion of cadherins to ECM proteins has not been noted in the literature. This may indicate non-physiological behavior of these VE-cadherin-coated beads.

Protein A coated beads unreacted with cadherin formed no attachment to beads that was able to withstand applied forces of 690 pN. These beads were not endocytosed, even after a 24 hour incubation. The lack of binding of Protein A beads to cells confirms that the cadherin coating on our beads was in fact interacting with the cells in binding specifically to cell-membrane cadherins.

3.3   Cell experiments

3.3.1 Magnetic trap experiments in wild-type HUVEC cells

The results of the bead pulling experiments on normal HUVECs are presented in

Figure 3.3. Half of the experiments were performed using 60 second timesteps for force

profiles 1 and 2, and the other half with the 110 second timesteps used in the rest of the

experiments. Use of a 110 second timestep for the rest of the experiments was chosen to

make the total time period of force application the same for the three force profiles. The

time of detachment was noted in the experiments using 110 second force profiles, and only

one cell detached after remaining adherent for the first 60 seconds of force application. This

leads us to consider data from the 60 second and 110 second timestep experiments in

aggregate.

Fisher's one-tailed exact test was used to compare detachment for beads subjected to

force profile 1 versus those subjected to force profile 2, and beads subjected to force profile 3

versus force profile 2. The null hypothesis was that the force profile applied did not affect

the probability of bead detachment. All the Fisher exact test calculated probabilities in this

paper were calculated using statistical software[63]. For force profile 1 versus force profile 2, p

= .0016 for, so the difference between detachment in response to constant low and constant

high force is statistically significant at a 95% confidence level ($p < 0.05$). For force profile 2

versus force profile 3, p = .1899, so the null hypothesis, that ramping the force does not have

an effect on bead detachment, cannot be rejected at a 95% confidence level. The probability

for force profile 1 vs profile 3 was 0.1704, indicating the difference between those profiles is

not statistically significant either.

3.3.2 Magnetic trap experiments in VASP-GFP-expressing HUVECs

Data from the bead pulling experiments on recombinant HUVECs expressing VASP-GFP and GFP-MITO-FPPPP are shown in Figure 3.4. All of these experiments were performed with 110 second timesteps. It was noted that the majority of beads detaching during force profile 3 did so at an intermediate force in the ramp, not at the highest force.

Fisher's one-tailed exact test was used to compare results between pairs of force profiles. Again, a null hypothesis proposing that force application did not affect the proportion of detaching beads was used. $p = 0.1022$ for comparison of force profile 1 and force profile 2, indicating the difference in bead detachment between these levels is not statistically significant at $p < 0.05$. For force profile 2 versus force profile 3, the probability of the null hypothesis being true is 0.1278, so the difference in the ramped versus constant high force profile is not statistically significant for for $p < 0.05$ either. Comparing force profile 1 to force profile 3 gives $p = 0.0042$, indicating that bead detachment for the two profiles is significantly different.

3.3.3 Magnetic trap experiments in GFP-MITO-FPPPP-expressing HUVECs

Figure 3.5 presents the data for bead pulling experiments on the HUVECs expressing the GFP-MITO-FPPPP construct. All of these experiments were performed with 110 second timesteps.

Comparison of the data from application of force profile 1 to force profile 2 via Fisher's one-tailed test yielded $p = 0.0012$, small enough to conclude that there is a significant difference at a 95% confidence level ($p < 0.05$) in the probability of a bead's detachment in response to constant low versus constant high force. However, the test gave $p = 0.4643$ for the comparison of force profile 2 and force profile 3, indicating that the force ramp does not change bead detachment at the high force in a statistically significant way.

The difference between bead response to force profile 1 and force profile 3 was significant, with p = 0.0038 for the null hypothesis.

3.3.4 Magnetic trap experiments in HUVECs treated with cytochalasin D

The results of the magnetic bead pulling experiments on HUVECs treated with 200 nM cytochalasin D are presented in Figure 3.6. All of these experiments were performed with 110 second timesteps.

Calculating probability of no significant difference between detachment due to force profile 1 versus force profile 2 using Fisher's one-tailed exact test yielded p = 0.0009, meaning application of low or high force affects the probability of bead detachment in a statistically significant way. Results from force profile 2 and force profile 3 were very similar to each other, with p = .6427 indicating only a 35% chance the force ramp has an effect on the bead detachment compared to the constant high force. Conversely, the results for profile 1 versus profile 3 were very different, with p = 0.0015 for the null hypothesis.

3.3.5 Comparison of recombinant cells and cytochalasin D treated cells to wildtype

For comparison purposes, all the data for wildtype HUVECs, VASP-GFP HUVECs, GFP-MITO-FPPPP HUVECs, and cytochalasin D treated HUVECs from Figures 3.2 – 3.6 are presented together in Figure 3.7. Table 3.2 summarizes the statistical information comparing force profile 1 to force profile 2 and force profile 3 to force profile 2 for each of the recombinant cell types and the cytochalasin D treated beads.

To see how the expression of the GFP-VASP and GFP-MITO-FPPPP constructs affected the bead attachment and adhesion strengthening responses as compared to wildtype cells, Fisher's one-tailed exact test was used to calculate the probability of no difference between the results for each force profile in the recombinant cells as compared to the same force profile in the wild type cells. Fisher's one-tailed exact test was also used to calculate

the probability of no difference between the cytochalasin D treated cells and wildtype cells for each force profile. These probabilities are presented in Table 3.3.

Smaller fractions of beads detached from GFP-VASP cells compared to wildtype cells for force profiles 1 and 2, but the differences are not statistically significant at for $p < 0.05$. Higher proportions of beads detached from GFP-MITO-FPPPP expressing cells compared to wildtype untreated cells when exposed to force profile 1 and 2. This difference is statistically significant for for $p < 0.05$ for force profile 2. Beads attached to cytochalasin D treated HUVECs detached in greater proportion than those attached to wildtype untreated HUVECs in response to force profile 1 and 2, but the differences were not statistically significant for $p < 0.05$.

Beads on GFP-VASP expressing cells and on GFP-MITO-FPPPP expressing cells exposed to force profile 3 detached in greater proportion than those attached to wildtype untreated HUVECs. The difference was statistically significant at for $p < 0.05$ for GFP-MITO-FPPPP cells. Beads on wildtype HUVECs treated with cytochalasin D also released in greater proportion compared to untreated wildtype HUVECs in response to force profile 3, and the difference was statistically significant for $p < 0.05$.

(a)
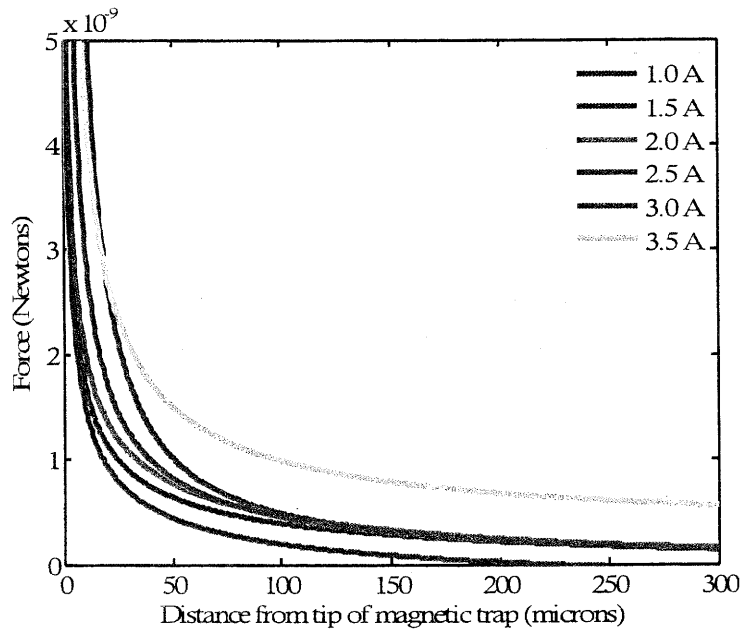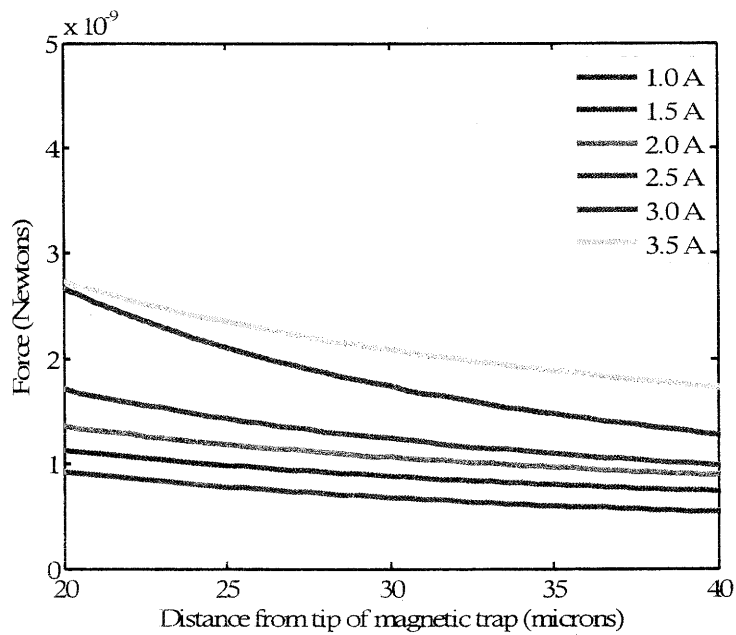

(b)

Fig. 3.1. **(a)** Power-law data regressions showing the force-current-distance relationship over 300 μm. **(b)** Closeup of the data regressions in the region near 30 μm, where bead pulling experiments were performed.
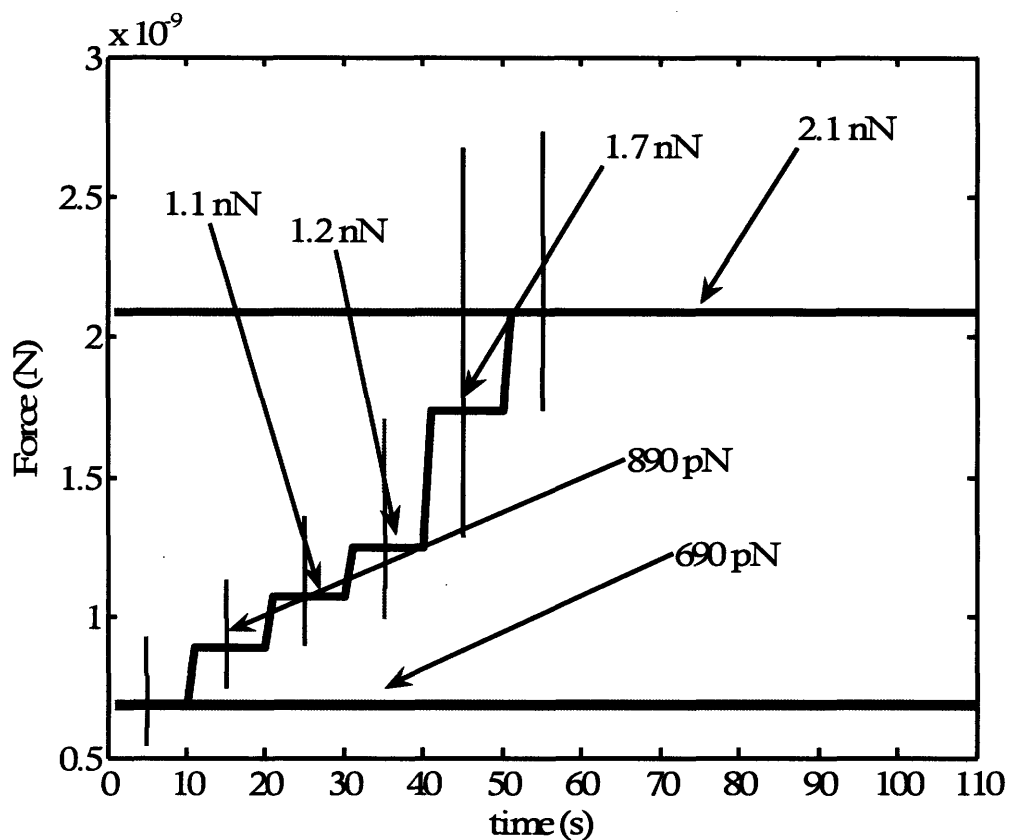
Fig. 3.2. The three different force profiles cell-adherent beads were subjected to in our

experiments. Force profile 1 (blue) subjected beads to a constant force of 690 pN, force

profile 2 (green) to a constant force of 2.1 nN, and force profile three ramped the force from

690 pN to 2.1 nN over fifty seconds and then held the peak force for 60 seconds. For each of

the six different force levels applied at a 30 μm distance from the bead, the pink error bars

show forces correlating to a ±5 μm difference from 30 μm in placement of the magnetic trap,

while the black error bars represent force levels over a ±10 μm distance.

Incubation time / Coating density	15 minutes	30 minutes	2 hours	24 hours
25%	No binding of beads to cells	Beads more responsive to high than low force	Beads more responsive to high than low force, some endocytosed beads	Beads endocytosed
50%	Timepoint not observed	Beads more responsive to high than low force, some endocytosed beads	Beads more responsive to high than low force, many endocytosed beads	Beads endocytosed
100%	Beads unresponsive to even >1 nN	Beads unresponsive to even >1 nN	Timepoint not observed (unresponsive beads assumed)	Beads endocytosed
Protein A	No binding or endocytosis	No binding or endocytosis	Timepoint not observed (no binding or endocytosis assumed	No binding or endocytosis

Table 3.1. Observations from preliminary experiments optimizing incubation period and density of cadherin coating on beads.
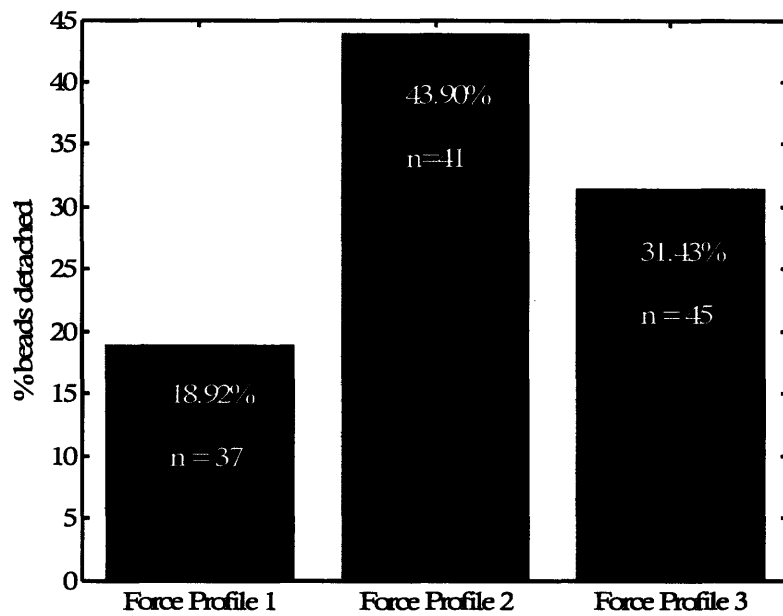
Fig. 3.3. Proportions of beads detached from wild-type untreated HUVECs in response to the different force profiles.
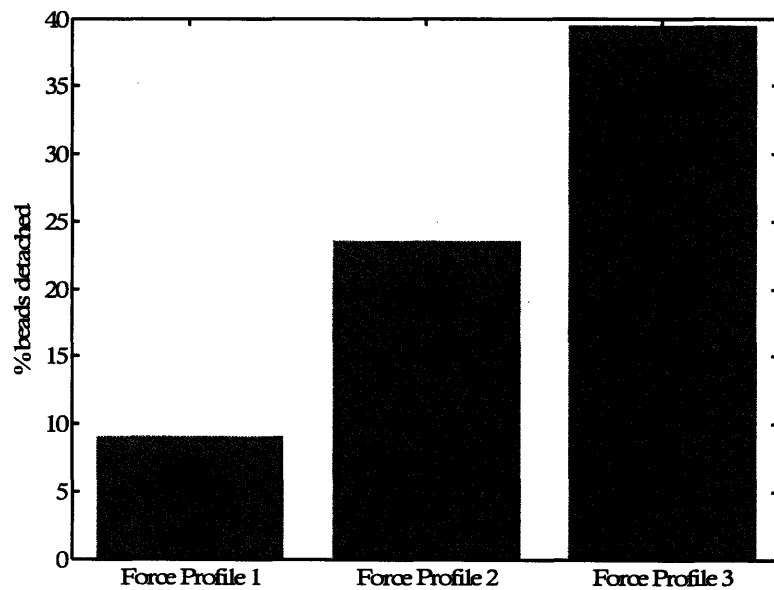

Fig. 3.4. Proportions of beads detached from GFP-VASP-expressing HUVECs in response to the different force profiles.
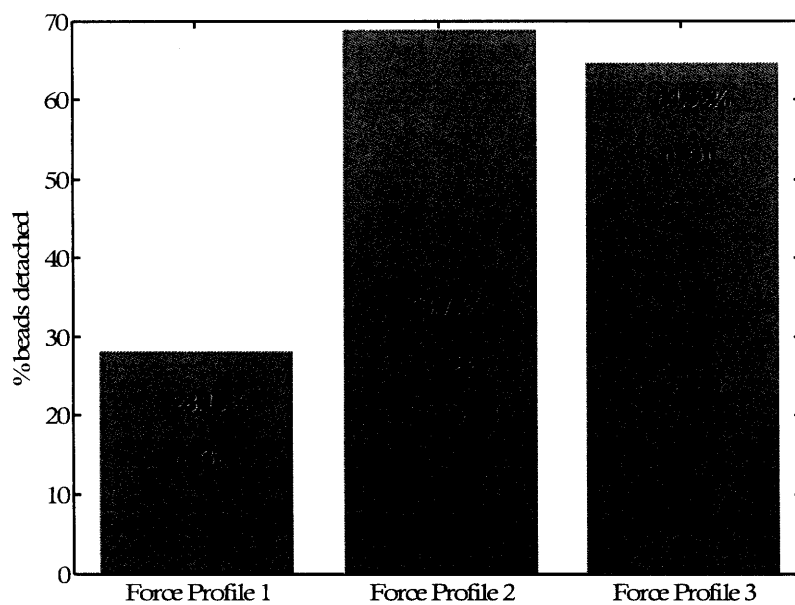
Fig. 3.5. Proportions of beads detached from GFP-MITO-FPPPP-expressing HUVECs in response to the different force profiles.
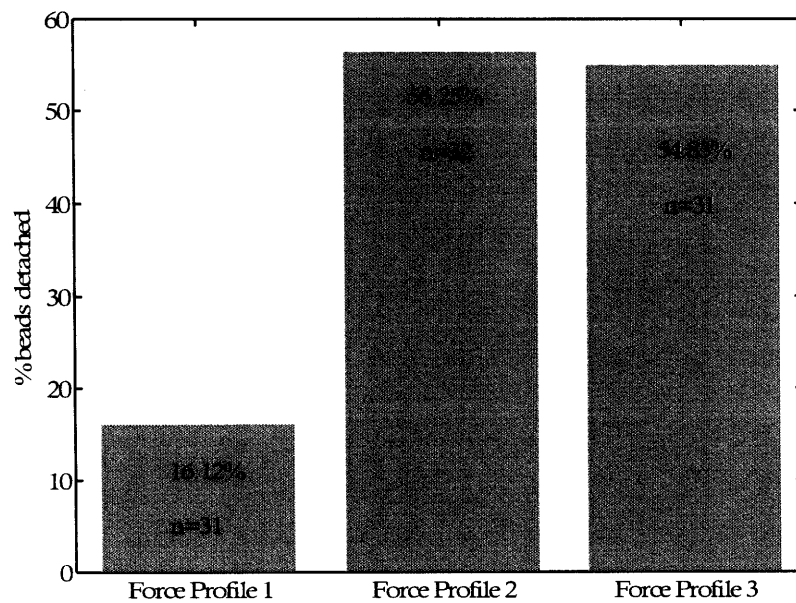
Fig. 3.6. Proportions of beads detached from wildtype cytochalasin D-treated HUVECs in response to the different force profiles.
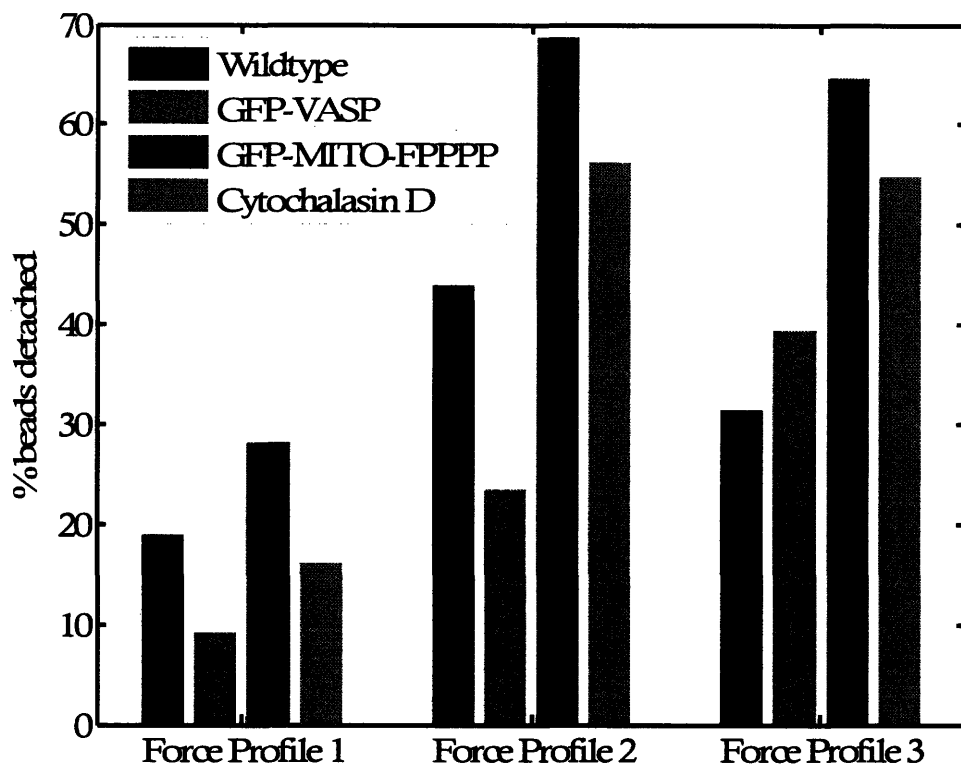
Fig. 3.7. Data from Figs. 3.2 – 3.6 presented side-by-side.

Cell type or treatment	Force Profile 1 vs Force Profile 2	Force Profile 2 vs Force Profile 3	Force Profile 1 vs Force Profile 3
Wildtype	0.0016	0.1899	0.1704
GFP-VASP	0.1022	0.1278	0.0042
GFP-MITO-FPPPP	0.0012	0.4643	0.0038
Cytochalasin D	0.0009	0.6427	0.0015

Table 3.2. The probabilities for the null hypothesis calculated from Fisher's one-tailed exact test are summarized. Highlighted cells indicate a statistically significant difference at a 95% confidence level.

| Cell
type or treatment	Force Profile 1	Force Profile 2	Force Profile 3
GFP-VASP	0.2042	0.0537	0.3325
GFP-MITO-FPPPP	0.2681	0.0295	0.0070
Cytochalasin D	0.5099	0.2088	0.0471

Table 3.3. Fisher's one-tailed exact test was used to calculate the probability of the null hypothesis, no difference between cell type or cytochalasin D treatment compared to wildtype cells, being true for each force profile. Highlighted cells indicate a significant difference ($p < 0.05$) between the indicated cell type or treatment and the wildtype results for that force profile.

4.0   Discussion

4.1   Adhesion strengthening in wildtype HUVECs

Cell-bound beads exposed to force profile 3 had a lower frequency of detachment

than beads exposed to force profile 2. The difference was not statistically significant at a

95% confidence interval, but was significant for an 80% confidence interval. The lower

frequency of detachment of beads which are exposed first to a force ramp implies that force-

responsive adhesion strengthening of the adherens junction may be occurring during that

force ramp, increasing the probability of the bead remaining adhered when exposed to a 2.1

nN force. Our hypothesis, that the strength of the cadherin-cadherin linkage increases in

response to the intermediate forces applied in the ramp , can be considered validated at an

80% confidence level but not at a 95% confidence level.

The difference in bead detachment in response to force profile 1 and force profile 2

was statistically significant. This merely indicates that the probability of bead detachment is

proportional to the force applied, as expected. The difference between response to force

profile 1 and force profile 3, however, was not significant at a 95% confidence interval. This

further indicates that adhesion strengthening may be occurring, as it shows the dependence

of detachment probability on force applied is not valid for beads pre-stressed with a ramping

force, but is valid for beads subjected to constant high force.

4.2   Adhesion strengthening in GFP-VASP expressing HUVECs

The cells expressing GFP-VASP, which behave like VASP-upregulated cells, show

less bead detachment in response to force profiles 1 and 2 as compared to the wildtype cells,

though the differences are not statistically significant at the 95% confidence level. Still, this

observed increase in the strength of cadherin-cadherin adhesion supports the hypothesis of

VASP-mediated actin regulation strengthening adherens junctions. VASP is known to localize to focal adhesions and adherens junctions and modulate the links between the cytoskeleton and the cell membrane. The greater strength with which GFP-VASP cells seem to hold beads could be the result of greater cytoskeletal linkage of cadherins.

Beads on GFP-VASP cells subjected to the ramped force profile detach in greater proportion than those subjected to constant high force, although the difference is not statistically significant. This result is contrary to our prediction of increased adhesion strengthening from VASP upregulation; the cells actually seem to experience "adhesion weakening" in response to ramped force.

The decrease in bead adhesion between force profile 2 and 3 may be related to the decrease in motility noted in fibroblasts with upregulated VASP. VASP upregulation and the resulting antagonism of capping proteins results in longer, more flexible actin filaments which also depolymerize at a greater rate due to Brownian dynamics (discussed in 1.3.3). Thus, by antagonizing capping protein, VASP upregulation may be acting to functionally increase the rate of unbinding of actin monomers to actin filaments. This could change the steady-state relationship of actin binding and unbinding to filaments, resulting in an overall slower growth of actin filaments. If actin linkages are strengthened in response to applied force, the slowed strengthening in VASP upregulated cells may make them unable to respond to force changes with appropriate cytoskeletal remodeling quickly enough, causing the bond to be broken.

This mechanism would explain why most of the beads detaching during force profile 3 detached during the ramp instead of at the highest force. It could also explain why fewer beads detached in response to a constant high force than to the ramp. In response to an initial force at an adherens junction, VASP creates links between the cytoskeleton and cadherin. The GFP-VASP cells make more links to the cytoskeleton due to the greater available pool of VASP. The antagonization of capping protein leads to inhibition of

cytosskeletal remodeling in response to changing force, explaining the increased detachment during the ramp.

4.3   Adhesion strengthening in GFP-MITO-FPPPP-expressing HUVECs

GFP-MITO-FPPPP-expressing cells showed a statistically significant difference in bead detachment response between constant low force and constant high force. In both cases, the fraction of detaching beads was greater than for wildtype cells subjected to the same force profile (with a statistically significant difference for force profile 2). This finding was in keeping with the hypothesis that delocalization of VASP from the cell membrane would lower the strength of bead adhesion. The fraction of beads detaching in response to force profile 3 was slightly lower than the fraction detaching in response to force profile 2, but not by a statistically significant difference. This, too, is in keeping with our hypothesis that VASP activity at adherens junctions is crucial in the adhesion strengthening response.

With this data and that from wildtype HUVECs and GFP-VASP expressing cells, a general profile of the role of VASP in force-mediated adhesion strengthening can be outlined. VASP is necessary for the formation of links between cadherin and the cytoskeleton, and VASP modulates these linkages in response to force. When VASP is downregulated, the initial cytoskeletal link is weaker, and strengthening of the link in response to force is also disabled. In the presence of upregulated VASP, the initial cytoskeletal link is stronger, but cannot adapt to increasing force due to the slowing of actin polymerization.

4.4   Adhesion strengthening in cytochalasin D-treated HUVECs

HUVECs treated with cytochalasin D showed no statistically significant difference from wildtype cells in response to constant low force or constant high force. The proportion of beads detaching from the cytochalasin D-treated HUVECs in response to ramped force is

almost the same as the proportion detaching from constant high force, showing that adhesion strengthening does not occur in these treated cells.

Previous experiments showed that fibroblasts treated with cytochalasin D drop in contractile force proportionally to the concentration of cytochalasin D[64]. Experiments in HUVECs showed that treatment with approximately 200 nM cytochalasin disrupted the actin cytoskeleton and removed most actin bundles[65]. Thus, the linkages between cadherin and the cytoskeleton are probably obliterated in these cells. These results indicate that the actin cytoskeleton is an important component of adhesion strengthening independently of simply forming initial linkages with cadherins at adhesion junctions. In response to a ramped force, wildtype cells must either create more linkages between the cytoskeleton and cadherin or increase the strength of existing linkages.

5.0   Conclusion

These experiments give further insight into the mechanisms of force-mediated adhesion strengthening at adherens junctions.   First, our experiments in wildtype cells monitoring bead detachment in response to constant high force and ramping force indicate that strengthening of adherens junctions in response to applied force does occur, as hypothesized, although our data validates this assertion at only an 80% confidence level.

The same experiments performed in VASP-upregulated and VASP-downregulated cells helped clarify some of the roles of VASP in adherens junctions. Beads attached to VASP-downregulated cells did not detach differently in response to constant high and ramped force, indicating that VASP is vital for the adhesion strengthening response. Cells with upregulated VASPs appeared to undergo "adhesion weakening" in response to ramped force, as a greater proportion of those beads detached compared to beads subjected to constant high force. This data suggested the importance of a controlled VASP concentration in creating cytoskeletal linkages and modulating the actin cytoskeleton. VASP strengthens the cadherin junction and promotes actin polymerization by inhibiting capping proteins. At high VASP concentrations, though, the promotion of actin polymerization may actually make the actin filaments less structurally stable and more likely to depolymerize, possibly slowing overall actin remodeling.

The experiments on cytochalasin-D treated wildtype HUVECs showed the effect of decoupling the actin cytoskeleton from cadherin on bead adhesion. The beads responded to low constant force and high constant force similarly to the way untreated wildtype cells did. The response of bead adhesion to a ramped force was the same as that to constant high force, suggesting that the actin cytoskeleton is a crucial element in adhesion strengthening, and possibly the only contributor of adhesion strengthening.

Given the importance of force application from neighboring cells on tissue structuring during development, it is conceivable that the activity of VASP is modulated during tissue development to allow cell polarization and organization within tissues. VASP activity could also contribute to cell behavior in pathological conditions. For instance, differential expression of VASP has been observed in normal lung tissue and lung adenocarcinomas. VASP expression is very low in normal lung tissue but upregulated in the cancerous cells[66]. As in our experiments, VASP upregulation in the lung cells may cause "adhesion weakening", leading to the decreased contact inhibition and increased cell motility seen in cancer cells. A better understanding of VASP activity regulation and its role in adhesion modulation will likely give information on both disease pathology and normal development. Our experiments show that cells respond to forces applied by neighboring forces with cytoskeletal remodeling, and the process is highly dependent on Ena/VASP proteins.

6.0   Future Work

The results of these experiments indicate that adhesion strengthening does occur at cell-cell contacts, and that VASP and the actin cytoskeleton play an important role in adhesion strengthening. However, these findings only scratch the surface of the complexities of adhesion strengthening. Many more experiments could be performed to understand better the mechanisms that drive adhesion strengthening works and the role of adhesion strengthening in physiology.

First of all, our experiments only validated adhesion strengthening in wildtype cells to a 80% level of confidence. A larger number of data points would increase the certainty of our conclusions about adhesion strengthening in wild-type cells, as well as our observations in the recombinant cell types and cytochalasin D. Additionally, a control experiment should be performed on cells transformed with a vector expressing a gene construct that does not associate with adherens junctions or the cytoskeleton. Gene transfection can affect the phenotype of other alleles besides the ones targeted. For instance, a cell transfected with a GFP construct could be used as a control.

At focal adhesions, separate processes contribute to adhesion strengthening. Cytoskeletal linkage, cell spreading to increase contact area with the ECM, and integrin recruitment to focal adhesions all play a role. It would be interesting to see if analogous processes contribute to adhesion strengthening at adherens junctions. Our experiments with cytochalasin D seemed to remove the contribution of cytoskeletal linkage to adhesion strengthening, although to verify that we did in fact do this, the adhesion strengthening response should be assessed in cells treated with different concentrations of cytochalasin D. Fluorescent probes for cadherin have been developed[67]; together with live cell imaging,

cadherin-coated beads and the magnetic trap, the cadherin recruitment response to applied force, if any, could be measured.

Live cell imaging could also be used to partially verify the theory developed from the data presented in this thesis that VASP associates with actin at adherens junctions in a force-dependent manner. Though force-dependent VASP association with actin has been noted at focal adhesions[68], it has not been investigated for adherens junctions. The GFP-VASP recombinant cells used in our experiments could be used with live cell imaging and magnetic trapping of cadherin-coated beads to determine if VASP association with actin at cell-cell junctions is force-dependent.

Another experiment probing the interaction of VASP with the cytoskeleton at adherens junctions would be to use cytoskeleton D to ablate the actin from GFP-VASP cells. If the increased strength of bead attachment for GFP-VASP HUVECs subjected to constant force profiles is due only to VASP creating more links with the cytoskeleton, then treatment with cytochalasin D should result in bead detachment data similar to that of wildtype HUVECs treated with cytochalasin D. Similarly, the "adhesion weakening" seen in GFP-VASP HUVECs subjected to ramped force should be eliminated as actin remodeling should no longer have any component to force. On the other hand, if GFP-VASP HUVECs treated with cytochalasin D do not behave like cytochalasin D-treated wildtype HUVECs, VASP is involved in other components of cell-cell binding and adhesion strengthening in addition to its functions in bridging cadherin to the cytoskeleton and modulating actin remodeling.

As discussed in 5.0, VASP modulation of cell-cell adhesion could be an important part of tissue development. By changing levels of VASP expression or activity in different tissues and at various stages of development, cells can organize and polarize within tissues to create specialized substructures. To test this hypothesis, mammalian tissue from various fetal development points could be isolated and the level of VASP at different stages of development analyzed via immunohistochemistry, Northern blotting, or DNA microarray.

Activation by PKA is needed for VASP to act at cell cell junctions[69], so the activity and expression of PKA may also be modulated over development.

VASP upregulation has been reported in cancerous tissues, and the results of our experiments suggest VASP upregulation alters cell-cell adhesion forces and adhesion strengthening response. The PKA inhibitor H89 increases permeability at endothelial junctions[69]; H89 also inhibits growth of cancerous cells in vitro[70]. Treatment with H89, or testing other ways of targeting VASP expression and activity, may be an effective method of reversing cancer phenotypes in cells. Identifying pharmacological modulators of VASP activity, and assessing their effect on cell-cell forces and adhesion strengthening, could be another pathway for new cancer therapies.

7.0   Acknowledgements

I owe much gratitude to Alisha Sieminski, who mentored me through this project at every step. Alisha initially suggested the problem, pointed me in the direction of relevant literature and helped me design my experiments, and offered suggestions on this thesis at every step. She exemplifies the creativity and dedication with which one should approach scientific problems. Thank you for all your inspiration and motivation.

Roger Kamm was my faculty advisor and was always available to discuss my results and offer creative suggestions for improvement. His encouragement, and Alisha's, kept me going when I felt entirely stuck by experimental setbacks. I really enjoyed working in the Kamm lab; the friendly, open, and challenging atmosphere has set the standard for my future scientific endeavors. Hayden Huang and Jan Lammerding, who designed the magnetic trap setup I used in these experiments, were very helpful in answering all of my questions about setting up my own experiments and troubleshooting problems.

Sid (Seok) Chung, a postdoctoral scholar in the Kamm lab, helped me design necessary adaptors in Solidworks for interfacing the micromanipulator to the magnetic trap. Arlis Reynolds, a graduate student in mechanical engineering, helped me construct those adaptors in the machine shop. I couldn't have done either task without their help. David Quinn, also a graduate student in mechanical engineering, provided vital help on several experiment needs, such as microscopy and video imaging, mounting the micromanipulator, and making the heating plate. David also provided lots of encouragement and mentorship and general camaraderie in the lab. He and the Suresh group kindly allowed me to use their microscope and video imaging setup.

My fellow students in the Kamm lab each helped me in some valuable way, whether it was suggesting a new direction for experiments, providing encouragement, or helping me order supplies. My fellow classmates in the Biological Engineering M.Eng program were

also encouraging throughout the process of creating this thesis, and collaborating with them during the required courses was fun. Finally, I couldn't have attended MIT at all without the support of my parents, and I am grateful for their encouragement of my scientific pursuits.

8.0 Appendices

Appendix A: Procedure For Coating Protein A Beads with Fc/VE-Cadherin (adapted from Ref. 55)

Needed reagents:

Buffer A: 100 mM Na phosphate, pH 8.1, (made from monosodium phosphate, 7892,

Mallinckrodt, Hazelwood, MO, and disodium phosphate, S373-500, Fisher Scientific,

Waltham, MA)

Buffer B: 200 mM triethanolamine, pH 8.2 (025K0170, Sigma, St. Louis, MO)

Buffer A with 0.1 µg/µL Fc/VE-cadherin

Buffer B with 5.4 µg/µL DMP (dimethyl pimelimidate dihydrochloride)

100 mM Tris, pH 7.5

1. Add 10 µL of protein A-coated beads to Eppendorf tube

2. Wash 3x in 100 µL buffer A:

      a. add buffer and suspend beads thoroughly

      b. use magnet to sediment beads

      c. decant buffer

3. Add 100 µL of buffer A containing dissolved Fc/VE-cadherin (0.1 µg/µL)

4. Tape tube to slow rocking platform and allow to react at room temperature for the length

of time determined by binding curve (Appendix B)

5. Wash 3x in 100 µL buffer B (as above with Buffer A)

6. Incubate beads for 45 minutes @ RT in 100 µL buffer B with DMP (5.4 µg/µL)

7. Sediment beads and decant DMP.

8. Wash 2x, 30 minutes each wash, with 100 µL 100 mM Tris,pH 7.5

9. Wash 3x 100 µL D-PBS with Ca, Mg

10. Store in 500 µL D-PBS with Ca, Mg at 4°C

Appendix B: Binding Curve for Fc domain to Protein A

The kinetics of binding of a ligand to a receptor-covered surface with no ligand

bound initially is given by

$$N_c = \frac{C_{L_o} N_{R_T}}{C_{L_o} + K_D} \left[1 - \exp(-k_{-1}(1 + \frac{C_{L_o}}{K_D})t) \right]$$ Eq. B.1

where N_c is the number of receptor-ligand complexes, C_{Lo} is the initial concentration of

ligand, k_{-1} is the dissociation rate coefficient, K_D is the equilibrium dissociation constant, N_{RT}

is the total number of receptors on the cell, and t is time[71].

The manufacturer does not supply information on the density of Protein A on their

beads, but using their specification that 100 µL of beads could absorb 25 µg of

immunoglobulin G from 100 µg/mL immunoglobulin G solution, and the area of the

baeads, a maximum number of receptor-ligand complexes, N_{cmax}, was calculated, 32051

µg/m² of bead surface area. $K_D = 0.6$ mg/mL and $k_{-1} = 0.072$ min⁻¹ were taken from

published data on protein A affinity to Fc[72], and N_{RT} calculated from the relation

$$N_{RT} = \frac{Nc_{max}(C_{Lo} + K_D)}{C_{Lo}} .^1$$ Eq. B.2

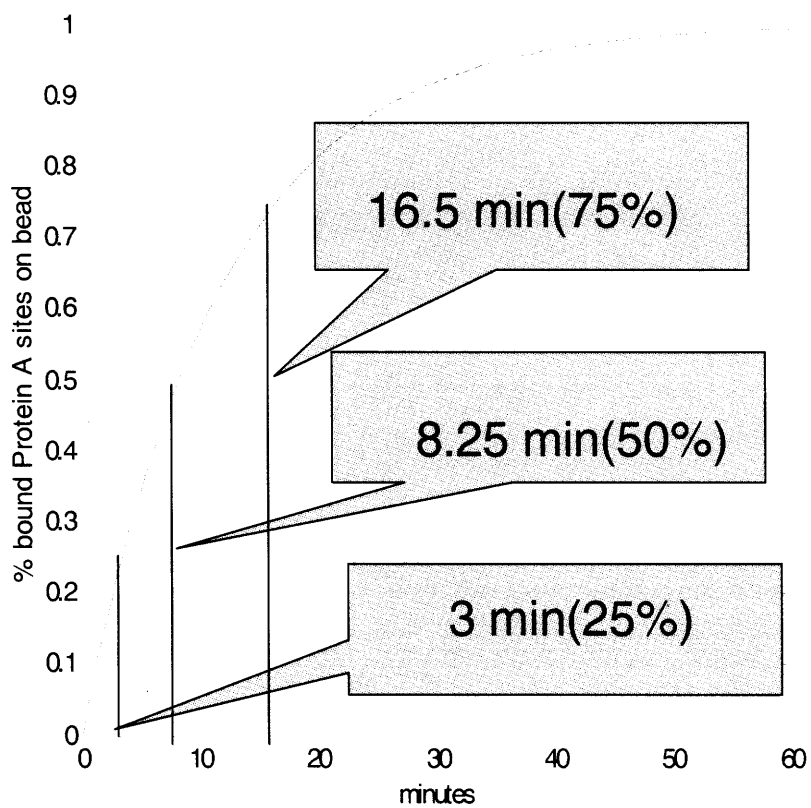Eq. B. 1. can then be plotted for N_c/N_{RT} as a function of time.

Fig. B.1. Binding curve for Fc domain to Protein A. Times indicated for creating the beads at the various densities. An incubation of 30 minutes was used to create "100%" cadherin coated beads, though the actual density is probably 92%.

Appendix C. Matlab programs for controlling power supply for force profiles

Creating serial port object and initializing:

```
s=serial('COM6')

fopen(s)
```

Force profile 1: constant_1A.m

```
set(s,'BaudRate',2400);

s.Terminator = 'CR/LF'

fprintf(s,'SI 0.00')

pause(1)

fprintf(s,'KOE')

pause(1)

fprintf(s,'SI 1.00')

pause(110)

fprintf(s,'KOD')
```

Force profile 2: constant_4A.m

```
set(s,'BaudRate',2400);

s.Terminator = 'CR/LF'

fprintf(s,'SI 0.00')

pause(1)

fprintf(s,'KOE')

pause(1)

fprintf(s,'SI 3.50')

pause(110)

fprintf(s,'KOD')
```

Force profile 3: ramp_10s_steps.m

```
set(s,'BaudRate',2400);

s.Terminator = 'CR/LF'

fprintf(s,'SI 0.00')

pause(1)

fprintf(s,'KOE')

pause(1)

fprintf(s,'SI 1.00')

pause(10)

fprintf(s,'SI 1.50')

pause(10)

fprintf(s,'SI 2.00')

pause(10)

fprintf(s,'SI 2.50')

pause(10)

fprintf(s,'SI 3.00')

pause(10)

fprintf(s,'SI 3.50')

pause(60)

fprintf(s,'KOD')
```

9.0   References

[1] Wang JH, Thampatty BP. An introductory review of cell mechanobiology. *Biomech Model Mechanobiol* 2006 Mar;5(1):1-16.

[2] Schoen FJ. Blood vessels. In: Kumar V, Abbas AK, Fausto N, editors. *Robbins and Cotran Pathologic Basis of Disease.* 7th ed. Philadelphia: Saunders, 2004. 512-14.

[3] Garcia-Cardeña G, Comander J, Anderson KR, Blackman BR, Gimbrone MA Jr. Biomechanical activation of vascular endothelium as a determinant of its functional phenotype.*Proc Natl Acad Sci USA* 2001;98(8):4478-85.

[4] Ziegler T, Silacci P, Harrison VJ, Hayoz D. Nitric oxide synthase expression in endothelial cells exposed to mechanical forces.*Hypertension* 1998;32(2):351-5.

[5] Davies, PF. How do vascular endothelial cells respond to flow? *News Physiol Sci* 1989;4:22-25.

[6] Punchard MA, Stenson-Cox C, O'cearbhaill ED, Lyons E, Gundy S, Murphy L, Pandit A, McHugh PE, Barron V.J Endothelial cell response to biomechanical forces under simulated vascular loading conditions. *J Biomech* 2007 Jun 8. Article in Press. doi:10.1016/j.jbiomech.2007.03.029

[7] Stevens T, Rosenberg R, Aird W, Quertermous T, Johnson FL, Garcia JG, Hebbel RP, Tuder RM, Garfinkel S. NHLBI workshop report: endothelial cell phenotypes in heart, lung, and blood diseases.*Am J Physiol Cell Physiol* 2001;281(5):C1422-33.

[8] Gumbiner BM. Cell adhesion: the molecular basis of tissue architecture and morphogenesis. *Cell* 1996;84:345-357.

[9] Chen CS, Tan J, Tien J. Mechanotransduction at cell-matrix and cell-cell contacts. *Annu Rev Biomed Eng* 2004;6:375-302.

[10] Wu MH. Endothelial focal adhesions and barrier function. *Physiology in Press* 2005;569(Pt 2):359-66.

[11] Lo SH. Focal adhesions: what's new inside. *Devl Biol* 2006;294:280-291.

[12] Vincent PA, Xiao K, Buckley KM, Kowalczyk AP. VE-cadherin: adhesion at arm's length. *Am J Physiol Cell Physiol* 2004;286:987-997.

[13] Nagafuchi A. Molecular architecture of adherens junctions. *Curr Opin Cell Biol* 2001;13:600-3.

[14] Garin G, Berk BC. Flow-mediated signaling modulates endothelial cell phenotype. *Endothelium* 2006;13(6) 375-84.

[15] Lehoux S., Castier Y, Tedgui A. Molecular mechanisms of the vascular responses to haemodynamic forces. *J Int Med* 2006;259(4):381-392.

[16] Chien S. Mechanotransduction and endothelial cell homeostasis: the wisdom of the cell. *Am J Physiol Heart Circ Physiol* 2007;292:H1209–H1224.

[17] Sawada Y, Sheetz MP. Force transductions by Triton cytoskeletons. *J Cell Biol* 2002;156(4):609-15.

[18] Domingos PP, Fonseca PM, Nadruz W Jr., Franchini KG. Load-induced focal adhesion kinase activation in the myocardium: role of stretch and contractile activity. *Am J Physio: Heart Circ Physiol* 2002;282:H556-64.

[19] Bryant P, Zheng Q, Pumiglia K. Focal adhesion kinase controls cellular levels of p27/Kip1 and p21/Cip1 through Skp2-dependent and -independent mechanisms.Mol Cell Biol. 2006;26(11):4201-13.

[20] Frisch SM, Vuori K, Ruoslahti E, Chan-Hui PY. Control of adhesion-dependent cell survival by focal adhesion kinase. *J Cell Biol* 1996;134:793-9.

[21] Chen CS, Mrksich M, Huang S, Whitesides GM. Micropatterned surfaces for control of cell shape, position, and function. *Biotechnol Progr.* 1998;14:356-63.

[22] Tan JL, Tien J, Pirone DM, Gray DS, Bhadriraju K, Chen CS. Cells lying on a bed of microneedles: An approach to isolate mechanical force. *Proc Natl Acad Sci USA* 2003;100(4):1484-9.

[23] Huang S, Chen CS, Ingber DE. Control of cyclin D1, p27Kip1 and cell cycle progression in human capillary endothelial cells by cell shape and cytoskeletal tension. *Mol Biol Cell* 1998;9:3179-93.

[24] Lo CM, Wang HB, Dembo M, Wang YL. Cell movement is guided by the rigidity of the substrate. *Biophys J* 2000;79:144-52.

[25] Wang HB, Dembo M, Hanks SK, Wang Y. Focal adhesion kinase is involved in mechanosensing during fibroblast migration. *Proc Natl Acad Sci USA* 2001;98:11295-300.

[26] Luo Y, Ferreira-Cornwell M, Baldwin H, Kostetskii I, Lenox J, Lieberman M, Radice G. Rescuing the N-cadherin knockout by cardiac-specific expression of N- or E-cadherin. *Development* 2001;128(4):459-69.

[27] Ko KS, McCulloch CAG. Intercellular mechanotransduction: cellular circuits that coordinate tissue responses to mechanical loading. *Biochem and Biophys Res Comm* 2001;285:1077-1083.

[28] Ganz A, Lambert M, Saez A, Silberzan P, Buguin A, Mége RM, Ladoux B. Traction forces exerted through N-cadherin contacts. *Biol Cell* 2006;98:721-30.

[29] Ragsdale GK, Phelps J, Luby-Phelps K. Viscoelastic response of fibroblasts to tension transmitted through adherens junctions. *Biophys J* 1997;73(5):2798-808.

[30] Ko KS, Arora PD, McCulloch CAG. Cadherins mediate intercellular mechanical signaling in fibroblasts by activation of stretch-sensitive calcium permeable channels. *J Biol Chem* 2001;276(38):35967-77.

[31] Chen CS, Tan J, Tien J. Mechanotransduction at cell-matrix and cell-cell contacts. *Annu Rev Biomed Eng* 2004;6:375-302.

[32] Iurlaro M, Demontis F, Corada M, Zanetta L, Drake C, Gariboldi M, Peiro S, Cano A, Navarro P, Cattelino A, Tognin S, Marchisio PC, Dejana E. VE-cadherin expression and clustering maintain low levels of survivin in endothelial cells. *Am J Path* 2004;165:181-9.

[33] Lotz MM, Burdsal CA, Erickson HP, McClay DR. Cell adhesion to fibronectin and tenascin: quantitative measurements of initial binding and subsequent strengthening response.
J Cell Biol 1989;109(4 Pt 1):1795-805.

[34] Gallant, N. Analysis of integrin-mediated cell adhesion strengthening using surfaces engineered to control cell shape and focal adhesion assembly. PhD diss., Georgia Institute of Technology, 2004.

[35] Choquet D, Felsenfeld DP, Sheetz MP. Extracellular matrix rigidity causes strengthening of integrin-cytoskeleton linkages. *Cell* 1997;88:39-48.

[36] Galbraith CG, Yamada KM, Sheetz MP. The relationship between force and focal complex development. *J Cell Biol* 2002;159(4):695-705.

[37] Riveline D, Zamir E, Balaban NQ, Schwarz US, Ishizaki T, Narumiya S, Kam Z, Bershadsky AD. Focal contacts as mechanosensorsL externally applied local mechanical force induces growth of focal contacts by a mDia1-dependent and ROCK-independent mechanism. *J Cell Biol* 2001;153(6):1175-1185.

[38] Wójciak-Stothard B, Potempa S, Eichholtz T, Ridley AJ. Rho and Rac but not Cdc42 regulate endothelial cell permeability. *J Cell Sci.* 2001;114(Pt 7):1343-55.

[39] Chu Y-S, Thomas WA, Eder O, Pincet F, Perez E, Theiry J-P, and Dufour S. Force measurements in E-cadherin-mediated cell doublets reveal rapid adhesion strengthening by actin cytoskeleton remodeling through Rac and Cdc42. *J Cell Biol* 2004;167(8):1183-94.

[40] Krause M, Dent EW, Bear JE, Loureiro JJ, Gerter FB. Ena/VASP proteins : regulators of the actin cytoskeleton and cell migration. *Annu Rev Cell Dev Biol* 2003;19:541-64.

[41] Gertler FB, Comer AR, Juang JL, Ahern SM, Clark MJ. Enabled, a dosage sensitive suppressor of mutations in the *Drosophila* Abl tyrosine kinase, encodes an Abl substrate with SH3 domain-binding properties. *Genes Dev* 1995;9:521-33.

[42] Krause M, Dent EW, Bear JE, Loureiro JJ, Gerter FB. Ena/VASP proteins : regulators of the actin cytoskeleton and cell migration. *Annu Rev Cell Dev Biol* 2003;19:541-64.

[43] Bear, JE, Svitkina, TM, Krause,M, Schafer, DA, Loureiro, JJ, Strasser, GA, Maly, IV, Chaga, OY, Cooper, JA, Borisy, GG, Gertler, FB. Antagonism between Ena/VASP proteins and actin filament capping regulates fibroblast motility. *Cell* 2002;109:509-521

[44] Trichet L, Campàs O, Sykes C, Plastino J. VASP governs actin dynamics by modulating filament anchoring. *Biophys J* 2007;92:1081-1089.

[45] Yoshigi M, Hoffman LM, Jensen CC, Yost HJ, Beckerle MC. Mechanical force mobilizes zyxin from focal adhesions to actin filaments and regulates cytoskeletal reinforcement. *J Cell Biol* 2005;171 (2):209-215.

[46] Howe AK, Hogan BP, Juliano RL. Regulation of vasodilator-stimulated phosphoprotein phosphorylation and interaction with Abl by protein kinase A and cell adhesion. *J Biol Chem* 2002;277:41(38121-38126),

[47] Geese M, Loureiro JJ, Bear JE, Wehland J, Gertler FB, Sechi AS. Contribution of Ena/VASP proteins to intracellular motility of Listera requires phosphorylation and proline-rich core but not F-actin binding or multimerization. *Mol Biol Cell* 2002;13:2383-96.

[48] Bear JE, Svitkina TM, Krause M, Schafer DA, Loureiro JJ, Strasser GA, Maly IV, Chaga OY, Cooper JA, Borisy GG, Gertler FB. Antagonism between Ena/VASP proteins and actin filament capping regulates fibroblast motility. *Cell* 2002;109(4):509-21.

[49] Krause M, Dent EW, Bear JE, Loureiro JJ, Gerter FB. Ena/VASP proteins : regulators of the actin cytoskeleton and cell migration. *Annu Rev Cell Dev Biol* 2003;19:541-64.

[50] Vasioukhin V, Bauer C, Yin M, Fuchs E. Directed actin polymerization is the driving force for epithelial cell-cell adhesion. *Cell* 2000;100(2):209-19.

[51] Scott JA, Shewan AM, den Elzen NR, Loureiro JJ, Gertler FB, Yap AS. Ena/VASP proteins can regulate distinct modes of actin organization and cadherin-adhesive contacts. *Mol Bio Cell* 2006;17:1085-95.

[52] Sieminski A., Massachusetts Institute of Technology, personal correspondence 8/2007.

[53] Bausch AR, Ziemann F, Boulbitch AA, Jacobson K, Sackmann E.Biophys J. Local measurements of viscoelastic parameters of adherent cell surfaces by magnetic bead microrheometry. *Biophys J* 1998;75(4):2038-49

[54] Mack PJ, Kaazempur-Mofrad MR, Karcher H, Lee RT, Kamm RD. Force-induced focal adhesion translocation: effects of force amplitude and frequency. Am J Physiol Cell Physiol 2004;287:C954-C-952.

[55] Baumgartner W, Golenhofen N, Grundhofer N, Wiegand J, Drenckhahn D. Ca+2 dependence of N-cadherin function probed by laser tweezer and atomic force microscopy. *J Neurosci* 2003;23(35)11008-11014.

[56] El Sayegh TY, Arora PD, Laschinger CA, Lee W, Morrison C, Overall CM, Kapus A, McCulloch CAG. Cortactin associates with N-cadherin adhesions and mediates intercellular adhesions strengthening in fibroblasts. *J Cell Sci* 2004;117:5117-5131.

[57]Brouxhon S, Kyrkanides S, O'banion MK, Johnson R, Pearce DA, Centola GM, Miller JN, McGrath KH, Erdle B, Scott G, Schneider S, Vanbuskirk J, Pentland AP. Sequential

Down-regulation of E-Cadherin with Squamous Cell Carcinoma Progression: Loss of E-Cadherin via a Prostaglandin E2-EP2 Dependent Posttranslational Mechanism. *Cancer Res* 2007;67(16):7654-64.

[58] Harhaja NS, Antonetti DA. Regulation of tight junctions and loss of barrier function in pathophysiology. Int J Biochem & Cell Biol 2004;7:1206-37.

[59] Lammerding, J. (2004). Quantitative analysis of subcellular biomechanics and mechanotransduction. PhD Thesis, Massachusetts Institute of Technology, Cambridge, MA.

[60] Rottner K, Krause M, Gimona M, Small JV, Wehland J. Zyxin is not colocalized with vasodilator-stimulated phosphoprotein (VASP) at lamellipodial tips and exhibits different dynamics to vinculin, paxillin, and VASP in focal adhesions. *Mol Biol Cell* 2001 Oct;12(10):3103-13.

[61] Personal correspondence, A. Sieminski.

[62] Disanza A, Mantoani S, Hertzog M, Gerboth S, Frittoli E, Steffen A, Berhoerster K, Kreienkamp HJ, Milanesi F, Di Fiore PP, Ciliberto A, Stradal TE, Scita G. Regulation of cell shape by Cdc42 is mediated by the synergic actin-bundling activity of the Eps8-IRSp53 complex. *Nat Cell Biol* 2006; 8(12):1337-47.

[63] Preacher, K. J., & Briggs, N. E. (2001, May). Calculation for Fisher's Exact Test: An interactive calculation tool for Fisher's exact probability test for 2 x 2 tables [Computer software]. Available from http://www.quantpsy.org.

[64] Wakatsuki T, Schwab B, Thomspon NC, and Elson EL. Effects of cytochalasin D and latrunculin B on mechanical properties of cells. *J Cell Sci* 2000;114:1025-1036.

[65] Chen J, Fabry B, Schiffrin EL, Wang N. Twisting integrin receptors increases endothelin-1 gene expression in endothelial cells. *Am J Physiol Cell Physiol* 2001;280: C1475-C1484.;

[66] Dertsiz L, Ozbilim G, Kayisli Y, Gokhan GA, Dermican A, Kayisli UA. Differential expression of VASP in normal lung tissue and lung adenocarcinomas. *Thorax* 2005;**60**:576-581.

[67] Adams CL, Chen YT, Smith SJ, Nelson WJ. Mechanisms of epithelial cell-cell adhesion and cell compaction revealed by high-resolution tracking of E-cadherin-green fluorescent protein. *J Cell Biol* 1998;142:1105-19.

[68] Yoshigi M, Hoffman LM, Jensen CC, Yost HJ, Beckerle MC. Mechanical force mobilizes zyxin from focal adhesions to actin filaments and regulates cytoskeletal reinforcement. *J Cell Biol* 2005;171 (2):209-215.

[69] Comerford KM, Lawrence DW, Synnestvedt K, Levi BP, Colgan SP. Role of vasodilator-stimulated phosphoprotein in PKA-induced changes in endothelial junctional permeability. *FASEB J* 2002;16:583-585

[70] Bockman S, Nebe B. The in vitro effects of H-89, a specific inhibitor of protein kinase A, in the human colonic carcinoma cell line Caco-2. Eur J Cancer Prevention. 2003;12(6)469-78.

[71] Truskey GA, Yuan F, Katz DF. Cell surface ligand-receptor kinetics and molecular transport within cells. In *Transport Phenomena in Biological Systems*. Upper Saddle River, NJ: Prentice Hall, 2004, 509-13.

[72] Tejada-Mansir A, Espinoza R, Montesinos RM, Guzman R. Modelling regeneration effects on protein A affinity chromatography. *Bioprocess Eng* 1997;17:39-44.